

Diamond nucleation by energetic pure carbon bombardment

Y. Yao,¹ M. Y. Liao,^{1,2} Th. Köhler,^{1,3} Th. Frauenheim,^{1,3} R. Q. Zhang,^{1,4} Z. G. Wang,² Y. Lifshitz,^{1,5,*} and S. T. Lee^{1,†}
¹Center of Super-Diamond and Advanced Films (COSDAF) and Department of Physics and Materials Science, City University of Hong Kong, Hong Kong SAR, China

²Key Lab of Semiconductor Materials Science, Institute of Semiconductors, Chinese Academy of Sciences, Beijing 100083, China

³Physik Department, Universität Paderborn, D-33098 Paderborn, Germany

⁴Nano-organic Photoelectronic Laboratory, Technical Institute of Physics and Chemistry, Chinese Academy of Science, Beijing 100101, China

⁵Department of Materials Engineering, Technion—Israel Institute of Technology, Haifa 32000, Israel

(Received 24 February 2005; published 1 July 2005)

Deposition of 1000 eV pure carbon ions onto Si(001) held at 800 °C led to direct nucleation of diamond crystallites, as proven by high-resolution transmission electron microscopy and electron energy loss spectroscopy. Molecular dynamic simulations show that diamond nucleation in the absence of hydrogen can occur by precipitation of diamond clusters in a dense amorphous carbon matrix generated by subplantation. Once the diamond clusters are formed, they can grow by thermal annealing consuming carbon atoms from the amorphous matrix. The results are applicable to other materials as well.

DOI: [10.1103/PhysRevB.72.035402](https://doi.org/10.1103/PhysRevB.72.035402)

PACS number(s): 81.05.Uw, 61.46.+w, 64.60.Qb, 81.15.Aa

The extreme properties of diamond coupled with its attractive applications^{1–3} initiated manmade synthesis of diamond via a high-pressure high-temperature process.⁴ Chemical vapor deposition (CVD) methods followed to make diamond at subatmospheric pressures and at ~ 800 °C.^{1–3} The most controlled method for diamond nucleation on foreign substrates is bias-enhanced nucleation^{5,6} (BEN) in which a hydrocarbon or hydrogen plasma is accelerated toward a 100–200 V negatively biased substrate. Comparable results can be obtained by direct ion bombardment of a mixture of hydrogen and carbon species.⁷ We recently⁸ proposed a model describing the nucleation of diamond from energetic bombardment of hydrogen- and carbon-containing species.

Deposition using energetic pure carbon ion bombardment has been investigated extensively.^{9–11} Amorphous diamond-like carbon (DLC) films with a sp^3 fraction of 0–90% and properties intermediate between graphite and diamond were reported⁹ and ordered sp^2 forms (graphites and carbon nanotubes^{12,13}) were prepared as well. It is widely accepted that the structure and properties of DLC films result from shallow implantation (subplantation).^{9–11} The sp^3 fraction is determined by the equilibrium between trapping in subsurface positions (densification) and detrapping (relaxation). The tuning of the carbon structure can be achieved through proper selection of carbon ion energy and substrate temperature. Nevertheless, all previous attempts to nucleate diamond by energetic pure carbon bombardment were unsuccessful.^{12,14}

This paper gives experimental evidence for diamond nucleation by bombardment of energetic (1000-eV) carbon ions with no hydrogen. This is in contrast with our previous model that attributes the diamond nucleation from a mixture of hydrogen and carbon energetic species to the crucial role of hydrogen. Moreover, using molecular dynamic (MD) simulations we present a model that explains the diamond nucleation and growth in a pure carbon environment and does not require hydrogen to remove the “thermodynamic

paradox” (Ref. 15) of diamond nucleation in subatmospheric conditions. Consequently the conditions for diamond nucleation are much broader and the mechanism of diamond growth is more diverse than previously believed.

Diamond nucleation was performed by mass-selected ion beam deposition (MSIBD). Carbon ions were accelerated from a CO₂-fed ion source, magnetically separated, and decelerated to bombard the Si (001) target held at 800 °C with energy of 1000 eV. The current density was 250 $\mu\text{A}/\text{cm}^2$ and the ion dose 2×10^{18} ions/cm². The hydrogen atomic concentration in the film according to elastic recoil detection analysis was much less than 1%. The film was characterized by high-resolution transmission electron microscopy (HRTEM; 200 keV Philips CM200 FEG with a point resolution of 0.19 nm). A Gatan spectrometer was used for transmission electron energy loss spectroscopy (EELS) to detect the elemental composition and the phase of the film.

The structure of amorphous carbon (*a*-C) matrices was studied using a nonorthogonal density-functional-based tight-binding (DFTB) scheme for fixed volume MD simulations.¹⁶ Our DFTB MD scheme was successfully applied to carbon and hydrocarbon structures.^{17–19} The method uses a minimal basis two-center approach to density-functional theory (DFT) for deriving total energies and interatomic forces. It provides an optimal compromise of accuracy and computational efficiency compared to full *ab initio* methods or to MD calculations using empirical potentials or semiempirical TB schemes. We used Γ -point Brillouin zone sampling for total energy calculations in sufficiently large three-dimensional (3D) periodic supercells. The cell size was 256 and 512 atoms. Two kinds of calculations were performed: (1) To study cluster precipitation, we started from a complete random distribution of atoms. Models of *a*-C in densities of 3.0, 3.3, and 3.5 g/cm³ (five models for each) have been cooled down from a complete random gaseous high-temperature initial structure of a given density by a stochastically driven dynamical quenching process following an

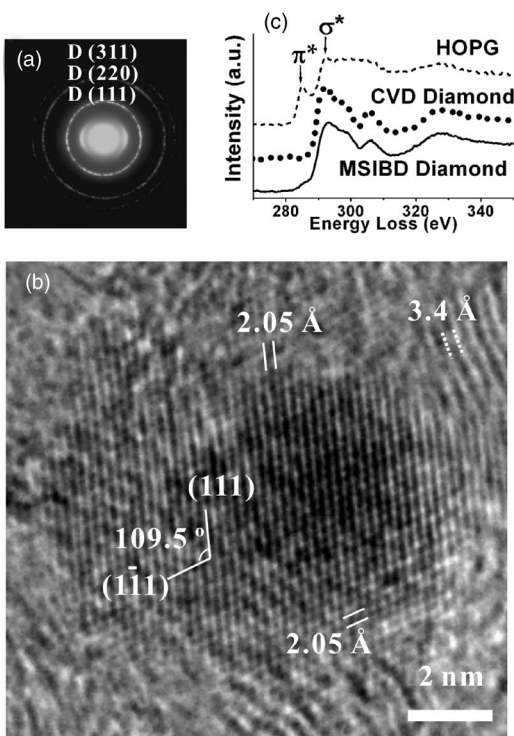


FIG. 1. (a) Cross-sectional SAED pattern of a region 80 nm away from the silicon substrate. Note the graphitic lobes, the diamond rings, and the absence of SiC spots; (b) A cross-sectional HRTEM image of the area corresponding to (a). A diamond crystallite embedded in a graphitic region is evident. The two diamond (111) planes intersect with an angle of 109.5° ; (c) Transmission EELS of the diamond crystallite in (b) (MSIBD diamond). The characteristic fine structure of diamond is evident by comparison to the EELS spectra of CVD diamond and HOPG.

exponential temperature path from 8000 to 300 K over 8 ps (mean cooling rate 10^{15} K/s). The low-energy amorphous structures were equilibrated at room temperature for another 0.5 ps with no significant further changes of structure. (2) To study diamond growth within an amorphous matrix we inserted a diamond seed of 66 atoms into a random gaseous initial structure of totally (seed+matrix) 512 carbon atoms. We cooled down these structures following an exponential temperature path over 8 ps from 5000 to 1000 K, while the last 2 ps toward 300 K were linearly quenched. This was done at densities of 2.0, 3.0, and 3.5 g/cm^3 . During simulation the seed was kept fixed. We additionally simulated *a*-C models of the same size and densities but without the forced diamond region to compare the energetic stability of amorphous systems at several densities with and without the injected diamond seed. Here the total exponential cooling path ran again over 8 ps from 8000 to 300 K.

Figure 1(a) shows the cross-sectional selected-area electron diffraction pattern (SAED) of the film at about 100 nm away from the substrate. The characteristic diamond pattern is easily recognized, along with oriented graphitic lobes. Figure 1(b) is a cross-sectional HRTEM image of the film from the same region analyzed in Fig. 1(a) showing three phases: graphitic fringes with a spacing of 0.34 nm, an amorphous (carbon) phase, and cubic diamond crystals with the

0.205-nm diamond spacing and the typical 109.5° angle between the cubic diamond (111) planes. HRTEM images of about 20 different diamond crystallites were obtained providing conclusive evidence for diamond nucleation in the *a*-C matrix. The similar edge and fine structure of the EELS spectra [Fig. 1(c)] of the crystallites in Fig. 1(b) and CVD diamond confirm both the carbon composition (pure carbon) and cubic diamond phase of the crystallites.

Our recent model⁸ describes diamond nucleation from energetic (hydrogen and carbon) species in terms of an internal (bulk) process occurring in subsurface layers and advancing as follows: (1) formation of a dense amorphous hydrogenated carbon (*a*-C:H) phase via subplantation, (2) spontaneous precipitation of pure sp^3 carbon clusters in the *a*-C:H phase, a few of which are perfect diamond clusters, (3) annealing of defects in the diamond cluster by incorporation of carbon interstitials and by hydrogen termination, (4) growth of the diamond cluster by preferential displacement of amorphous carbons at the diamond/amorphous carbon interface, some of which occupy diamond positions, while the diamond atoms remain intact.

Our experimental data and MD calculations lead us to propose a diamond nucleation and growth model distinctively different from our previous one due to the different deposition conditions used (a pure carbon source vs a mixture of carbon and hydrogen species): (1) Formation of a dense, pure, amorphous carbon (*a*-C) phase. (2) Spontaneous precipitation of pure sp^3 carbon clusters in the *a*-C phase, a few of which are perfect diamond clusters. Appropriate nucleation sites (e.g., graphitic edges) enhance precipitation of perfect diamond. (3) Growth of diamond crystallites by consumption of *a*-C atoms from the surrounding dense matrix due to enhanced density fluctuations upon thermal annealing. Preferential displacements by bombarding ions play a secondary role.

Let us now discuss each step in detail. Deposition of carbon by pure, mass-selected 1000-eV species is a subplantation process in which carbon is incorporated in subsurface positions. The penetration and bombardment of energetic ions lead to densification. The pure carbon film thus deposited is expected to be denser than one containing 20% hydrogen (>2.8 g/cm^3). We thus assume that for energetic pure carbon deposition the density of the precursor *a*-C matrix in which diamond nucleates is fluctuating around 3–3.5 g/cm^3 .

We further study the spontaneous precipitation of pure sp^3 clusters (step 2) in *a*-C models obtained by dynamical stochastic quenching at densities of 3.0, 3.3, and 3.5 g/cm^3 . In one of 15 MD calculations performed (five for each density) on a cell of 256 carbon atoms and a density of 3.5 g/cm^3 we demonstrate the precipitation of a defective diamond cluster of 41 atoms (Fig. 2). The electronic density of states of this cluster [Fig. 2(b)] shows a band gap >5 eV as expected for diamond. Diamond clusters may also precipitate in *a*-C with a smaller density, e.g., 3 g/cm^3 . We detected pronounced nanoscale density fluctuations between 2.5 to 3.5 g/cm^3 in MD simulations of *a*-C structures with an average density of 3 g/cm^3 at increased cell sizes of 512 atoms. We observed the formation of large amorphous 100% sp^3 clusters of 60 to 100 atoms each embedded in a lower density carbon matrix.

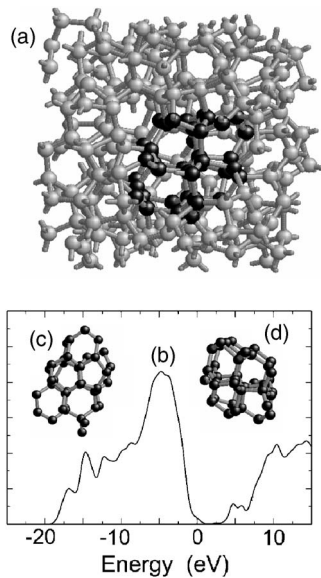


FIG. 2. (a) A 3.5-g/cm^3 $a\text{-C}$ cell with 256 carbon atoms from DFTB MD calculations. The diamondlike cluster of 41 atoms formed by annealing and rapid cooling has the electronic density of state of diamond (b), and is shown at different projections in (c) and (d).

The spontaneous generation of 100% sp^3 clusters (a small fraction of which may be diamond clusters) for densities lower than 3.5 g/cm^3 needs large-cell simulations to be detected. Significantly, the precipitation of a diamond cluster in the present case of a pure, hydrogen-free, $a\text{-C}$ matrix is enhanced and stabilized only by the dense matrix that serves as a mold. Fyta *et al.*²⁰ have recently shown that the total energy of a dense $a\text{-C}$ matrix is reduced by introduction of a diamond cluster. We believe this is the driving force for the precipitation of diamond clusters in a dense $a\text{-C}$ matrix. The probability for diamond precipitation in pure $a\text{-C}$ should be smaller than that in an $a\text{-C:H}$ matrix, where the cluster is additionally stabilized by hydrogen termination. Indeed, we detected only one faulty diamond cluster in 15 models of pure $a\text{-C}$, though in all of them we could observe nanoscale density fluctuations yielding 100% sp^3 clusters of a reasonable size. The probability of diamond clustering might be increased by nucleation sites. Several different diamond nucleation sites have been discussed in the literature including graphitic edges,²¹ carbon nano-onions,²² silicon steps,²³ and silicon carbide.²⁴ Our HRTEM images confirm the precipitation of at least some diamond crystallites on graphitic edges and onionlike structures, but no diamond nucleus was detected in the present work on the silicon substrate or on silicon carbide sometimes formed on the silicon substrate.

To address the diamond growth in step 3 we investigated the thermal annealing of the diamond cluster in an $a\text{-C}$ matrix driven by the boundary conditions superimposed by the surrounding matrix (“mold effect”).¹¹ MD calculations of a 66-atom diamond seed introduced to a 512-cluster in a 3.5 g/cm^3 (Fig. 3) and 3 g/cm^3 (not shown here) $a\text{-C}$ matrix show that the cluster grows upon annealing. The growth is more efficient in the $[110]$ direction in an $a\text{-C}$ matrix with a density of 3.5 g/cm^3 and is less oriented for the growth in the 3.0

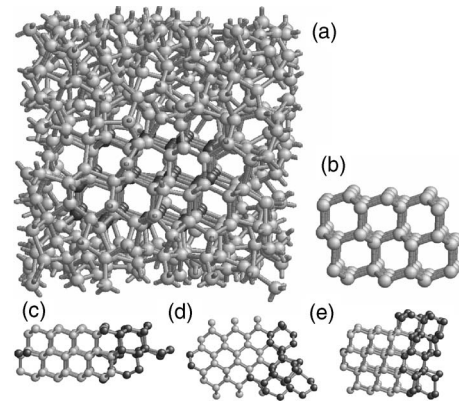


FIG. 3. DFTB MD calculations of a fixed diamond seed of 66 atoms embedded in a 3.5-g/cm^3 $a\text{-C}$ cell. (a) The cell with the embedded seed (total 512 carbon atoms) at the end of a cooling down process; (b) the original 66-atom diamond seed; (c)–(e) three projections of the grown seed (40 atoms added, mainly in the $[110]$ direction).

-g/cm^3 matrix. The growth is energetically more favorable (by about 18 eV) and efficient for the less dense matrix, probably due to the smaller stress induced by expansion of the diamond crystal. The energy gain by introducing the diamond seed to the $a\text{-C}$ cell (compared to a pure $a\text{-C}$ cell of the same size) is 32.5 eV for a density of 3 g/cm^3 and only 14.8 eV for a density of 3.5 g/cm^3 . However, a minimal density is needed for the diamond cluster growth, as no growth was observed in an $a\text{-C}$ matrix of 2 g/cm^3 . Growth by thermal annealing is possible also by BEN, but is less likely due to the smaller density. On the other hand, hydrogen termination assists in thermal annealing of defects in faulty diamond clusters (in BEN), whereas radiation damage is difficult to anneal in a hydrogen-free pure carbon matrix.

The diamond growth mechanism we proposed for BEN (Ref. 8) was preferential displacement of loosely bonded $a\text{-C}$ atoms at the $a\text{-C:H}$ –diamond interface, leaving the diamond atoms intact. This mechanism is less likely for pure carbon bombardment than for BEN. The total number of displacements of each carbon atom due to ion bombardment in the present case (3–10) is much smaller than for BEN (30–100). This reflects the overall effect of the larger number of displacements per atom ($\sim 3\text{--}10$ for pure 1000-eV C compared to $\sim 0.3\text{--}1$ for BEN) but the low ion to C atom arrival ratio (1 for C ions, ~ 100 for BEN). Additionally the increased ion energy needed for diamond nucleation by pure carbon deposition is, however, large enough to displace the diamond atoms suppressing the diamond crystal growth by radiation damage.

Diamond nucleation by ion bombardment of hydrogen-rich species is known for a decade.^{5,6} Here we demonstrate that pure carbon ion bombardment involving no hydrogen leads to diamond nucleation as well. The role of hydrogen in diamond nucleation is threefold:⁸ (1) enhancement of the probability of spontaneous nucleation of a diamond cluster and its stabilization, (2) assistance in annealing of defects in faulty diamond crystallites, and (3) preferential displacement of $a\text{-C}$ atoms by energetic hydrogen species leading to diamond crystallite growth. In a pure carbon matrix all

hydrogen-induced effects are absent and alternative factors are needed to promote diamond nucleation and growth. Two such factors are the density (larger than for that BEN) and the temperature. The density provides the boundary conditions necessary for: (1) spontaneous precipitation of diamond clusters and (2) the further growth of diamond crystallites. The temperature increases the carbon mobility necessary for annealing of defects and growth. The ion energy required for the formation of the dense matrix is deleterious to the growth of perfect crystals due to radiation damage. The nucleation and growth environment provided by pure carbon bombardment is thus inferior to that by BEN.

The diamond nucleation in the absence of hydrogen indicates that the mold effect (the boundary conditions superimposed by the surrounding matrix) is strong enough to promote both nucleation and growth. The nucleation is enhanced by a sufficient density, whereas the growth by the combined effect of density and temperature. The main positive bombardment effect (enhancing diamond nucleation and growth) in the present case is the generation of the dense precursor matrix. Some local modification might be introduced during the “thermalization stage” (Ref. 11) in which the excess energy in the excited region along the track of the penetrating ion is dissipated in the matrix. The relaxation during this stage, often denoted as the “thermal spike,” (Ref. 11) is treated by MD calculations (we assume a rapid annealing to 8000 K (~ 0.7 eV) and a following rapid cooling at a rate of 10^{15} K/s in a period of $\sim 10^{-11}$ s in accord with the energies and time scale involved in our MSIBD scheme). Thermal effects during the long-term relaxation stage (not treated by the MD simulations) may be much more efficient

in matrix relaxation than the “thermal spike” (Ref. 9). This means that annealing of the diamond cluster may even be more effective than predicted by our calculations. Despite the relaxation during thermal spike it seems that pure carbon bombardment for nucleation and growth invariably introduces collisional damages, which are essentially deleterious to the development of high-quality diamond crystallites. The route to an optimized diamond nucleation process via pure carbon ion bombardment seems to be a reduction of ion energy and an increase of substrate temperature (either during deposition or by post deposition annealing).

In summary, energetic pure carbon bombardment results in the nucleation of diamond crystallites as evident from HRTEM characterizations. MD calculations show that diamond nucleation can occur in the absence of hydrogen by precipitation of diamond clusters in a dense *a*-C matrix. Further simulations show that once the diamond clusters are formed, they can grow by thermal annealing consuming carbon atoms from the amorphous matrix. This process is essentially different from diamond nucleation and growth in a hydrogen-rich environment of energetic carbon species. It manifests the important role of the boundary conditions of the surrounding matrix on the nucleation and growth of diamond and other materials as well.

This work is supported by the Chinese Academy of Sciences and the Special Funds for Major State Basic Research Project No. G20000683, China, a Central Allocation Grant (CityU 2/04C) of the Research Grants Council of HKSAR, and by the Bundesministerium für Bildung und Forschung, Germany.

*Corresponding author. Electronic address: apshay@cityu.edu.hk

†Corresponding author. Electronic address: appannale@cityu.edu.hk

¹J. C. Angus, C. C. Hayman, *Science* **241**, 643 (1988).

²*The Physics of Diamond*, edited by A. Paoletti and A. Tucciarone, International School of Physics “Enrico Fermi” Course 135 (IOS, Amsterdam, 1997).

³*Diamond Films: Recent Developments*, edited by D. M. Gruen and I. Buckley-Golder, special issue of *MRS Bull.* **23**(9), (1998).

⁴F. P. Bundy, H. T. Hall, H. M. Strong, and R. H. Wentorf, Jr., *Nature (London)* **176**, 51 (1955).

⁵S. Yugo, T. Kanai, and T. Muto, *Appl. Phys. Lett.* **58**, 1036 (1991).

⁶X. Jiang, C.-P. Klages, R. Zachai, M. Hartweg, and H.-J. Fusser, *Appl. Phys. Lett.* **62**, 3438 (1993).

⁷W. J. Zhang, X. S. Sun, H. Y. Peng, N. Wang, C. S. Lee, I. Bello, and S. T. Lee, *Phys. Rev. B* **61**, 5579 (2000).

⁸Y. Lifshitz, T. Kohler, T. Frauenheim, I. Guzman, A. Hoffman, R. Q. Zhang, X. T. Zhou, and S. T. Lee, *Science* **297**, 1531 (2002).

⁹Y. Lifshitz, *Diamond Relat. Mater.* **8**, 1659 (1999).

¹⁰Y. Lifshitz, S. R. Kasi, and J. W. Rabalais, *Phys. Rev. Lett.* **62**, 1290 (1989).

¹¹Y. Lifshitz, S. R. Kasi, J. W. Rabalais, and W. Eckstein, *Phys. Rev. B* **41**, 10468 (1990).

¹²S. T. Lee and S. Chen, *Appl. Phys. Lett.* **59**, 785 (1991); **60**, 2213 (1992).

¹³H. Y. Peng, N. Wang, Y. F. Zheng, Y. Lifshitz, J. Kulik, R. Q. Zhang, C. S. Lee, and S. T. Lee, *Appl. Phys. Lett.* **77**, 2831 (2000).

¹⁴W. M. Lau, I. Bello, X. Feng, L. J. Huang, Qin Fuguang, Yao Zhenyu, Ren Zhizhang, and S. T. Lee, *J. Appl. Phys.* **70**, 5623 (1991).

¹⁵J. C. Angus, in *The Physics of Diamonds* (Ref. 2), pp. 20–21; P. Badziag, W. S. Verwoerd, W. P. Ellis, and N. R. Greiner, *Nature (London)* **343**, 244 (1990).

¹⁶G. Seifert and E. Eschrig, *Phys. Status Solidi B* **127**, 573 (1985).

¹⁷D. Porezag, M. R. Pederson, T. Frauenheim, and T. Köhler, *Phys. Rev. B* **52**, 14963 (1995).

¹⁸T. Frauenheim, G. Jungnickel, Th. Köler, U. Stephan, and Th. Köhler, *J. Non-Cryst. Solids* **182**, 186 (1995).

¹⁹T. Frauenheim, G. Jungnickel, U. Stephan, P. Blaudeck, S. Deutschmann, M. Weiler, S. Sattel, K. Jung, and H. Ehrhardt, *Phys. Rev. B* **50**, 7940 (1994).

²⁰M. G. Fyta, I. N. Remediakis, and P. C. Kelires, *Phys. Rev. B* **67**, 035423 (2003).

²¹W. R. L. Lambrecht, C. H. Lee, B. Segall, J. C. Angus, Z. Li, and

- M. Sunkar, *Nature (London)* **364**, 607 (1993).
- ²²F. Banhart, *Rep. Prog. Phys.* **62**, 1181 (1999).
- ²³S. T. Lee, H. Y. Peng, X. T. Zhou, N. Wang, C. S. Lee, I. Bello,
and Y. Lifshitz, *Science* **287**, 104 (2000).
- ²⁴R. Stöckel, M. Stämmler, K. Janischowsky, L. Ley, M. Albrecht, and H. P. Strunk, *J. Appl. Phys.* **83**, 531 (1998).